

1 **TRITEX: chromosome-scale sequence assembly of Triticeae genomes with**
2 **open-source tools**

3
4 **Cécile Monat¹, Sudharsan Padmarasu¹, Thomas Lux², Thomas Wicker³, Heidrun Gundlach²,**
5 **Axel Himmelbach¹, Jennifer Ens⁴, Chengdao Li^{5,6}, Gary J. Muehlbauer⁷, Alan H. Schulman⁸,**
6 **Robbie Waugh⁹, Ilka Braumann¹⁰, Curtis Pozniak⁴, Uwe Scholz¹, Klaus F. X. Mayer^{2,11},**
7 **Manuel Spannagl², Nils Stein^{1,12}, Martin Mascher^{1,13}**

8
9 ¹Leibniz Institute of Plant Genetics and Crop Plant Research (IPK) Gatersleben, Seeland,
10 Germany

11 ²PGSB – Plant Genome and Systems Biology, Helmholtz Center Munich – German Research
12 Center for Environmental Health, Neuherberg, Germany

13 ³Department of Plant and Microbial Biology, University of Zurich, Zurich, Switzerland

14 ⁴Department of Plant Sciences, University of Saskatchewan, Saskatoon, Canada

15 ⁵Western Barley Genetics Alliance, School of Veterinary and Life Sciences (VLS), Murdoch
16 University, Murdoch, WA, Australia

17 ⁶Hubei Collaborative Innovation Center for Grain Industry / School of Agriculture, Yangtze
18 University, Jingzhou, China

19 ⁷Department of Agronomy and Plant Genetics & Department of Plant and Microbial Biology,
20 University of Minnesota, St. Paul, Minnesota, USA

21 ⁸Green Technology, Natural Resources Institute (Luke), Viikki Plant Science Centre, and
22 Institute of Biotechnology, University of Helsinki, Helsinki, Finland

23 ⁹The James Hutton Institute, Dundee, UK & School of Life Sciences, University of Dundee,
24 Dundee, UK

25 ¹⁰Carlsberg Research Laboratory, Copenhagen, Denmark

26 ¹¹School of Life Sciences Weihenstephan, Technical University of Munich, Germany

27 ¹²Department of Crop Sciences, Center for Integrated Breeding Research (CiBreed), Georg-
28 August-University Göttingen, Göttingen, Germany

29 ¹³German Centre for Integrative Biodiversity Research (iDiv) Halle-Jena-Leipzig, Leipzig,
30 Germany

31
32 Correspondence should be addressed to Martin Mascher (mascher@ipk-gatersleben.de) or
33 Nils Stein (stein@ipk-gatersleben.de).

34

35 **Abstract**

36

37 Chromosome-scale genome sequence assemblies underpin pan-genomic studies. Recent
38 genome assembly efforts in the large-genome Triticeae crops wheat and barley have relied
39 on the commercial closed-source assembly algorithm DeNovoMagic. We have developed
40 TRITEX, an open-source computational workflow that combines paired-end, mate-pair, 10X
41 Genomics linked-read with chromosome conformation capture sequencing data to construct
42 sequence scaffolds with megabase-scale contiguity ordered into chromosomal
43 pseudomolecules. We evaluated the performance of TRITEX on publicly available sequence
44 data of tetraploid wild emmer and hexaploid bread wheat, and constructed an improved
45 annotated reference genome sequence assembly of the barley cultivar Morex as a
46 community resource.

47

48 **Introduction**

49

50 The Triticeae species wheat and barley were among the founder crops of Neolithic
51 agriculture in Western Asia and continue to dominate agriculture in temperate regions of
52 the world to the present day. Large genome sizes, high content of transposable elements
53 (TEs) and polyploidy (in the case of wheat) have long impeded genome assembly projects in
54 the Triticeae [1, 2]. Recently, chromosome-scale reference sequence assemblies have come
55 available for barley (*Hordeum vulgare*) [3], hexaploid bread wheat (*Triticum aestivum*) [4],
56 tetraploid durum wheat (*T. turgidum* ssp. *durum*) [5] as well as the wheat wild relatives
57 *Aegilops tauschii* (wheat D genome progenitor) [6], *T. urartu* (wheat A genome progenitor)
58 [7] and *T. turgidum* ssp. *dicoccoides* (wild emmer wheat, AB genome) [8]. The genome
59 projects of barley, bread wheat and the A and D genome progenitors had initially followed
60 the hierarchical shotgun approach as had been employed by the human genome project [9],
61 but adopted second-generation sequencing methods for sequencing as they became
62 available [10]. Assembling bacterial artificial chromosomes (BACs) guided by a physical map
63 yielded megabase-sized scaffolds [3, 11], which were then arranged into chromosomal
64 super-scaffolds (so-called “pseudomolecules”) by long-range linkage information afforded by
65 ultra-dense genetic maps [12, 13], chromosome conformation capture sequencing (Hi-C) [14,
66 15] or Bionano optical mapping [16]. However, BAC-by-BAC assembly is laborious and time-
67 consuming [3], and has become an obsolete method of sequence assembly.

68 The wild emmer wheat, and subsequently the bread and durum wheat, genome projects [4,
69 5, 17] used a whole-genome shotgun (WGS) approach based on Illumina short-read
70 sequencing of shotgun libraries with multiple insert sizes. Within months, a fully annotated,
71 highly contiguous sequences was assembly, capturing the full organizational context of the
72 21 wheat chromosomes, some of which have been validated using other approaches [18].
73 Despite being robust, the assembly algorithm used in these projects was closed-source [19],
74 potentially limiting its application to the broader community. Indeed, efforts to develop a
75 low-cost, open source alternative are still required to allow assembly of multiple genomes
76 within a species to comparable contiguity. Short-read assemblies of the wheat genome have
77 been generated by open-source alternatives such as w2rap [20] or Meraculous [13]. In
78 addition, long-read assemblies have been generated for *Ae. tauschii* [21] and bread wheat
79 [22]. But still the contiguity of these assemblies is lower than that of the scaffolds
80 constructed using the DeNovoMagic algorithm. Another important concern is the high
81 computational cost for a long-read (hybrid) assembly, estimated at 470,000 CPU hours or 6.5
82 months in wall-clock time [22].

83 We have recently outlined a proposal for pan-genomics in barley [23]. A cornerstone of our
84 strategy is the construction of high-quality sequence assemblies for multiple genotypes
85 representative of major germplasm groups. Similar projects are under way in bread wheat
86 (<http://www.10wheatgenomes.com>). An open-source assembly pipeline with comparable
87 accuracy, completeness and speed similar to available commercial platforms would greatly
88 reduce the cost per assembled genome, thus extending the scope of pan-genome projects in
89 the Triticeae.

90 Here, we report on the development of a computational pipeline for chromosome-scale
91 sequence assembly of wheat and barley genomes. We evaluate the performance of the
92 pipeline (which we named TRITEX) by re-assembling the raw data used for the wild emmer
93 [8] and bread wheat [24] reference genome assemblies and compare our assemblies to the
94 those constructed with a commercial platform. Furthermore, we used TRITEX to generate an

95 improved annotated reference genome assembly for barley cv. Morex as an important
96 resource for the barley research community.

97

98 **Results**

99

100 *Overview of the workflow*

101

102 We begin with a description of our workflow, its input datasets (**Table 1**) and a description of
103 the expected outcome of each component (**Table 2**). For the sake of exposition, we illustrate
104 our method by presenting results for wheat and barley, which will be described in greater
105 detail below.

106 Our pipeline uses the same input datasets generated for DeNovoMagic assemblies reported
107 by Avni et al. [17] and the International Wheat Genome Sequencing Consortium (IWGSC) [4].
108 The key parameters are two types of paired-end libraries (PE450 and PE800), three types of
109 mate-pair libraries (size ranges: 2-4 kb [MP3], 5-7 kb [MP6] and 8-10 kb [MP9]), 10X
110 Chromium libraries, and Hi-C data as listed in **Table 1**. We show below that certain library
111 types can be omitted in our approach without greatly compromising assembly contiguity.

112 A critical component of the “sequencing recipe” are PCR-free Illumina shotgun libraries with
113 a tight insert size distribution in the range of 400-500 bp and sequenced with 250 bp paired-
114 end reads. These were merged with standard tools such as PEAR [25] or BBMerge [26] to
115 yield long single-end reads with a mean fragment size of ~450 bp and are subsequently
116 error-corrected with BFC [27]. These elongated short reads allow the use of longer k-mers
117 (i.e. short sequence fragments of fixed length) during the assembly process. Estimates of
118 expected assembly size based on k-mer cardinalities [28] support the notion that longer k-
119 mers achieve much better genome representation in wheat and barley (**Fig. 1a**). The k-mer
120 size for many assemblers is limited. For example, the maximum k-mer size of SOAPDenovo2
121 is limited to 127 bp. We thus selected Minia3 [29, 30], an assembler capable of using k-mers
122 of arbitrary size.

123 However, one disadvantage of using large k-mer sizes is the lower genome coverage (**Fig. 1b**)
124 as a consequence of sequencing errors, resulting in random coverage gaps. To overcome this
125 drawback, we adopted the iterative multi k-mer approach of the GATB-Minia pipeline
126 <https://github.com/GATB/gatb-minia-pipeline>). In the initial iteration, an assembly at k-mer
127 size 100 is made from the error-corrected PE450 reads. Subsequent iterations take as input
128 the PE450 reads and assembly constructed in the previous iteration. This procedure is
129 repeated for k-mer sizes 200, 300, 350, 400, 450 and 500. The unitigs of the final iteration
130 achieve an N50 of about 20 – 30 kb (**Table 3**). A single iteration takes about one day for
131 barley and three days for hexaploid wheat.

132 The unitigs of the final iteration are used as input for scaffolding with the PE800, MP3, MP6
133 and MP9 libraries using SOAPDenovo2 [6]. This yields assemblies with an N50 beyond 1 Mb
134 (**Table 3, 4**). After gap-filling with GapCloser, about 1 – 5 % internal gaps in scaffolds remain
135 (**Tables 3, 4**). Alignments of 10X and Hi-C reads and genetic markers to the scaffolds are
136 imported into R [31] and custom scripts were developed to identify and correct mis-
137 assemblies, to construct super-scaffolds and to build pseudomolecules. Both super-
138 scaffolding with 10X data and pseudomolecule construction use the POPSEQ genetic maps of
139 barley [12] and wheat [13] to guide the assignment of scaffolds to chromosomes and to
140 discard spurious links between unlinked regions. We note that the omission of the PE800,
141 MP3 and MP6 libraries (i.e. using only the MP9 library for mate-pair scaffolding) resulted in
142 assemblies of comparable contiguity and genome representation in barley (**Table 4**). If this

143 slightly reduced contiguity is acceptable for downstream application, the cost for data
144 generation can be reduced by about 20%.

145 Scaffolding can introduce false joins between unlinked sequences [32] that need to be
146 broken to construct correct chromosomal pseudomolecules [33]. Physical coverage with 10X
147 reads is used to detect and correct mis-joins introduced during either unitig construction or
148 scaffolding (Fig. 2). The corrected scaffolds are used as input for super-scaffolding with 10X
149 data using a custom graph-based method (see Methods section for details). These super-
150 scaffolds are then ordered and oriented along the chromosomes using Hi-C data using the
151 method of Beier et al. [34]. Once scaffolds have been arranged into chromosomal
152 pseudomolecules, contact matrices for each chromosome are plotted as heat maps. Visual
153 inspection of these matrices can reveal further assembly errors such as remaining chimeras
154 or misoriented (blocks of) super-scaffolds (Fig. 3). After correction of these errors, the Hi-C
155 maps are updated and cycles of assembly-inspection-correction are repeated until all mis-
156 assemblies have been eliminated and contact matrices show the expected Rabl
157 configuration [3] (strong main diagonal / weak anti-diagonal). We found that
158 pseudomolecules constructed from corrected super-scaffolds contain in the range of 10 to
159 20 mis-assemblies, which were eliminated in a single correction cycle. Without 10X data, i.e.
160 using only Hi-C data for spotting misassemblies as in the case of published wheat reference
161 genomes [4, 17], more curation cycles were required.

162 Assuming all input datasets (Table 1) are in place, the entire TRITEX workflow can be
163 completed in three to four weeks for barley and four to six weeks for hexaploid wheat,
164 allowing for some delays in the completion of hands-on steps (mainly inspection of
165 intermediate results and curation of pseudomolecules). We believe that despite our detailed
166 user guide (available at <https://tritexassembly.bitbucket.io>), completing a TRITEX assembly
167 would be a rather arduous task for a scientist inexperienced in either plant genome
168 assembly or practical bioinformatics, unless guided by an expert in plant genomics. A UNIX
169 server with at least 1 TB of main memory is needed to complete scaffold construction for
170 bread wheat. Much wall-clock time (about 1 week for barley [5 Gb genome] and about 3
171 weeks for bread wheat [16 Gb genome]) is spent for unitig assembly with Minia3.
172 Fortunately, the main memory consumption of Minia3 is low (50 GB). Thus, assemblies of
173 multiple genotypes (a typical use case in a pan-genome project) can be run in parallel.

174
175 *Re-assembly of wild emmer and bread wheat and comparison to published assemblies*
176

177 We downloaded the paired-end and mate-pair reads used for the DeNovoMagic assemblies
178 of wild emmer wheat accession Zavitan [17] and bread wheat cultivar Chinese Spring [4]
179 (referred to as the IWGSC whole-genome assembly in Table S2 of [4]) and ran TRITEX until
180 the gap-filling step (step 2 in Table 2). The metrics of TRITEX assemblies were inferior to
181 those of DeNovoMagic (Table 3). Still, the contiguity of the TRITEX assemblies was in the
182 megabase range, and it was clearly superior to the BAC-by-BAC assembly of a single wheat
183 chromosome (3B [11], N50: 892 kb). Visual inspection of alignments between the TRITEX and
184 DeNovoMagic assemblies indicated a high concordance between them (Fig. 4). To assess the
185 accuracy of the TRITEX assemblies at a genome-wide scale, we compared the TRITEX
186 scaffolds to published assemblies produced by the DeNovoMagic algorithm. These
187 assemblies had been independently validated by complementary sequence and mapping
188 resources [4, 17, 35]. We divided the TRITEX scaffolds into non-overlapping 10 kb fragments,
189 aligned them to the DeNovoMagic assemblies with Minimap2 [36] and measured the
190 collinearity of the alignments. The average Pearson correlation of fragment positions in the

191 TRITEX scaffold and their aligned positions in the DeNovoMagic scaffolds was 0.998 for
192 Chinese Spring and 0.999 for Zavitan. Across all Chinese Spring (Zavitan) scaffold pairs with
193 at least 100 kb of aligned sequences, 99.96 % (99.99 %) of aligned fragment sequences were
194 mapped in the same orientation. These results support a very high concordance in the local
195 order and orientation of sequences between the TRITEX and previous assembly efforts.
196 To assess the completeness of the TRITEX assembly of Chinese Spring, we determined the
197 representation of two transcript resources: the IWGSC gene models [4] and the full-length
198 cDNAs of Mochida et al. [37]. The proportion of completely represented transcripts in the
199 TRITEX assembly was very similar to the IWGSC RefSeq and substantially higher than in the
200 w2rap assembly [20] and the PacBio hybrid assembly of Zimin et al. [22] (**Table 5**). Note that
201 the IWGSC RefSeq gene models are likely to have a bias for the TRITEX assembly, which was
202 generated from the same input data, but it is not evident how the Sanger-sequenced full-
203 length cDNAs might favor a certain assembly.
204 A comparison of the TRITEX assemblies of Zavitan and Chinese Spring in comparison to their
205 published counterparts revealed a higher proportion of sequence gaps (**Table 3**). We
206 speculate that sequence gaps may arise because highly similar copies of transposable
207 elements (TEs) cannot be resolved. To test this hypothesis, we analyzed the representation
208 of two TE families, RLC_Angela and RLC_Sabrina [38], in the TRITEX and IWGSC WGA
209 assemblies of Chinese Spring. Despite having similar assembly sizes (**Table 3**), we identified
210 substantially fewer full-length RLC_Angela elements in the TRITEX assembly, whereas the
211 numbers of RLC_Sabrina elements matched closely in both assemblies (**Table S1**).
212 RLC_Angela is considered a recently active (i.e. transposing) family, whereas RLC_Sabrina
213 has been inactive for a long time (Thomas Wicker, unpublished results). Consistent with the
214 expectation that younger elements, which inserted recently and have highly similar copies
215 elsewhere in the genomes, are not well assembled, the age distribution of RLC_Angela is
216 skewed for older elements. By contrast, no such bias is seen for RLC_Sabrina (**Figure S1**). In
217 summary, the TRITEX assembly of Chinese Spring has fewer complete TEs, indicating that the
218 DenovoMagic algorithm may make better use of mate-pair or PE450 data to close gaps in
219 TEs.
220

221 *An improved barley reference genome assembly*

222 Prompted by the encouraging assembly results for wheat, we decided to employ the TRITEX
223 pipeline to construct a second version reference genome assembly of barley cv. Morex. The
224 need for an improved assembly arose from shortcomings of the BAC-based reference
225 sequence [3] including (1) large sequence gaps, (2) redundancies and (3) local mis-
226 assemblies.

227 First, gaps in the physical map or failed BAC assemblies result in gaps in the assembled
228 sequence that may contain important genes. During the process of pseudomolecule
229 construction [34], we attempted to “rescue” missed genes by adding sequences from a WGS
230 draft assembly of Morex [39]. However, the short WGS contigs do not provide the local
231 sequence context of genes and may not even contain full-length gene sequences. Second, it
232 was necessary to merge sequences from individually assembled BAC clones [10]. during
233 pseudomolecule construction [34]. Megabase-sized sequence scaffolds representing physical
234 contigs of BACs were constructed using a complex, multi-tiered method that employed
235 heuristic approaches to distinguish true sequence overlaps from alignments caused by highly
236 similar copies of transposable elements [34]. Nevertheless, self-alignment of the
237 pseudomolecule at a high identity threshold (minimum alignment length: 5 kb, minimum

239 alignment identity: 99.5 %) resulted in a substantial proportion (4.4 %) of undetected
240 overlaps between adjacent BACs. Similar results were obtained for the first version of the
241 BAC-based maize reference genome [40] (1.2 %) and the 3B pseudomolecule of Choulet et
242 al. [11] (7.4 %) using the same alignment thresholds.

243 Third, individual BAC clones were rarely represented by a single sequence scaffold even after
244 scaffolding with mate-pair data [10]. At the time barley BAC sequencing was performed,
245 methods with a sufficient density and resolution to order and orient sequence scaffolds
246 within 100 kb were not available. Hence, our solution [34] was to place sequence scaffolds
247 originating from the BAC clone in arbitrary order and orientation into the pseudomolecule,
248 thus introducing many local assembly errors at the sub-BAC scale.

249 Our results in wheat led us to expect that a TRITEX assembly of the Morex genome would
250 overcome the limitations inherent to the BAC-by-BAC approach. To construct a TRITEX
251 assembly of the Morex genome, we obtained the datasets as detailed in **Table 1**. New
252 paired-end, mate-pair and 10X libraries were constructed and sequenced. The Hi-C data of
253 Mascher et al. [3] were used for pseudomolecule construction. The assembly metrics of the
254 Morex TRITEX assembly greatly exceeded those of the BAC-by-BAC assembly. Notably, the
255 proportion of completely aligned full-length cDNAs improved by about nine percentage
256 points (**Table 4**) compared to the BAC-by-BAC assembly.

257 To ascertain the correct local order and orientation of sequence scaffolds, we compared the
258 TRITEX super-scaffolds to three complementary resources: (i) the first version (V1)
259 pseudomolecules, (ii) the BAC-by-BAC assembly improved by super-scaffolding based on
260 newly collected in-vitro proximity ligation and (iii) the genome-wide optical map of Morex.
261 First, visual inspection of alignments confirmed the expected discordances at the sub-BAC
262 level, but showed good collinearity at the megabase-scale (**Fig. 5a**). We used the same
263 approach as for the comparison to the published wheat assemblies by aligning 10 kb
264 fragments. The Pearson correlation between TRITEX fragments and their aligned positions in
265 the Morex V1 pseudomolecules was 0.927, reflecting a breakdown of collinearity at finer
266 resolution. The orientations in the pseudomolecules of fragments originating from the
267 TRITEX super-scaffolds was highly discordant: on average, only 63 % of aligned sequence in
268 TRITEX/Morex V1 scaffold pairs was in concordant orientation.

269 Second, we compared the TRITEX super-scaffolds to an improved version of the BAC-by-BAC
270 assemblies of Mascher et al. [3]. Before the development of TRITEX, we had attempted to
271 order and orient BAC sequence scaffolds using the Dovetail method. This involved in-vitro
272 proximity ligation sequencing (Chicago) followed by scaffolding with the HiRise assembler
273 [41]. Visual inspection of alignments between TRITEX super-scaffolds and Dovetail scaffolds
274 revealed a higher concordance compared to the V1 pseudomolecules (**Fig. 5a, b**). At the
275 level of 10-kb fragment alignments, the collinearity between TRITEX positions and mapped
276 position in the Dovetail assembly was 0.982 (Pearson correlation). On average, 94.8 % of
277 aligned sequence in TRITEX/Dovetail scaffold pairs was concordant orientation. We note that
278 the Dovetail assembly was based on the same sequence scaffolds generated from single
279 assembled BAC clones as were used in the Morex V1 pseudomolecule. Hence, the issues of
280 sequence gaps due to failed BAC assemblies and artificial duplication persist. Nevertheless,
281 Dovetail scaffolding did improve the presentation of complete full-length cDNAs by about
282 two percentage points (**Table 4**), most likely by mending occasional sequence breaks within
283 genes.

284 Third, we compared the TRITEX super-scaffolds to the optical map of the Morex genome
285 constructed by Bionano genome mapping [3, 16]. The optical contigs were aligned to the *in*
286 *silico* digested TRITEX assembly using Bionano's Refaligner. Of Nt.BspQ1 sites in the

287 assembly, 95.9 % were covered by high-confidence alignments (score ≥ 20) of optical
288 contigs and 88.6 % of label sites were aligned. Vice versa, 95.3 % of label sites in the Bionano
289 map were spanned by high-confidence alignments and 90.0 % of Bionano label sites were
290 aligned to the sequence assembly. Label sites covered by alignments, but themselves not
291 aligned (red lines in **Fig. 5c**) may be due to missed label sites in the optical map, gaps in the
292 sequence assembly or alignment uncertainties. We note that it was not possible to align
293 optical contigs to the BAC-based sequence scaffolds as their contiguity is too low (N50: 79
294 kb, **Table 4**, [34]). In summary, all three comparisons support the high local accuracy of the
295 TRITEX assembly.

296 To assess the accuracy at the pseudomolecule level, we plotted alignments between
297 chromosomal pseudomolecules of Mascher et al. ([3], Morex V1) and those constructed
298 using TRITEX (Morex V2) and inspected Hi-C contact matrices (**Fig. 6**). The V1 and V2
299 pseudomolecules were highly collinear. The contact matrices showed the expected Rabl
300 pattern. Several smaller mis-assemblies present in the V1 pseudomolecule were corrected in
301 V2. For example, Morex V1 had a misplaced sequence in the peri-centromeric regions of
302 chromosome 4H (300 – 400 Mb, **Fig. 6c**), which was correctly placed in Morex V2 as
303 supported by the Hi-C contact matrix (**Fig. 6b**).

304 The amounts and characteristics of repetitive sequences such as TEs and tandem repeats
305 represented in sequence assemblies can serve as proxies for assembly quality. We compared
306 the Morex V1 and V2 assemblies according to five criteria: (i) overall TE composition; (ii)
307 presence of highly abundant 20-mers; (iii) amount and localization of tandem repeats; (iv)
308 the amount and age distribution of retrotransposons; and (v) sequence gaps in selected TE
309 families. Overall TE composition was almost identical between the assembly versions (**Table**
310 **S2**). The chromosomal distribution of highly abundant 20-mers was similar in the Morex V1
311 and V2 assemblies, but Morex V2 contains more repetitive sequence in peri-centromeric
312 regions (**Fig. S3a**). Similarly, the Morex V2 assembly contains 50 % more tandem repeats
313 than V1. Notably, the number of satellite tandem repeats is almost doubled. Tandem
314 repeats are concentrated in short sequence scaffolds not assigned to chromosomes (chrUn)
315 in Morex V1 and at distal ends of several chromosomes (short arm of 4H, long arms of 4H
316 and 6H) and in peri-centromeric regions (**Fig. S3b**).

317 The representation of long-terminal repeat (LTR) retrotransposon families was similar in
318 both assemblies (**Table S2**). However, the Morex V2 assembly contains 1,590 (5 %) more
319 intact full-length elements than V1 (**Table S3**, **Fig. S2a, b**). In both assemblies, the number of
320 retrieved full-length LTRs matches the expectation based on genome size (**Fig. S2c**). Insertion
321 age distributions show that the Morex V2 assembly resolved a higher number of younger
322 *Copia* elements (**Fig. S2d**). The distinct peak at age 0 in the V1 assembly is most likely caused
323 by a scaffolding artefact from the chromosomal pseudomolecule construction when
324 sequences from the same BAC were arranged in arbitrary order in the Morex V1
325 pseudomolecules as described above. To understand the impact of sequence gaps on TE
326 representation in the Morex V2 assembly, we performed a similar analysis as for Chinese
327 Spring, using the recently active BARE1 family. The Morex V2 assembly contains more full-
328 length elements than V1 (5,471 vs. 3,469; **Table S1**). Moreover, the percentage of full-length
329 copies that are flanked by a target site duplication (TSD) is higher in the V2 assembly (90%
330 vs. 81%), suggesting fewer chimeric sequences. However, the size distribution of the
331 elements in the Morex V2 assembly indicates a large population of overly large full-length
332 elements (**Table S4**). In contrast, the size distribution of full-length elements in Morex V1 is
333 narrower and shows two characteristic peaks corresponding to the autonomous and non-
334 autonomous subfamilies (T. Wicker, unpublished results). Manual inspection of 50 randomly

335 selected elements between 9,900 and 10,000 bp in length showed that the large sizes of
336 these elements are mainly due to large sequence gaps (i.e. long stretches of N's). In the 50
337 manually inspected copies, we found 70 sequence gaps in the internal domain and only 5
338 short gaps in the LTRs. The latter observation is not surprising as our method to identify full-
339 length copies relied on largely gap-free LTRs. In only three cases, the large size of the
340 element was caused by the genuine insertion of additional TEs. Overall, the Morex V2
341 assembly had more and larger gaps as TE length increased (**Table S4**), a pattern that is
342 absent from the Morex V1 assembly. In summary, the representation of repetitive sequence
343 is similar in both assembly version of the Morex genome. The longer read lengths and k-mer
344 sizes used in the TRITEX pipeline may have resulted in a better representation of short
345 tandem repeats in V2. However, the gap-free assembly of very recently inserted full-length
346 TEs may benefit from prior complexity reduction such as BAC sequencing.
347 To facilitate the adoption of the Morex V2 assembly as a common reference sequence by
348 the cereal research community, we annotated the pseudomolecules using the same
349 transcript datasets as used by Mascher et al. [3] for Morex V1, but with an improved version
350 of the PGSB annotation pipeline. A total of 32,787 high-confidence (HC) and 30,871 low-
351 confidence (LC) gene models were annotated on the V2 pseudomolecules. Of the 1,440
352 BUSCOs (Benchmarking Universal Single-Copy Orthologs, [42]), 98.9 % were completely
353 represented by annotated genes, a 6.4 % increase compared to the V1 annotation. At the
354 same time, the V2 annotation has fewer high-confidence gene models (32,787 [V2] vs.
355 39,734 [V1]), likely owing to higher assembly contiguity (i.e. fewer fragmented gene
356 models), more stringent thresholds during the annotation process and the incorporation of
357 TE annotations as hints for *ab initio* prediction to reduce the number of transposon-related
358 genes. In a comparison against an independent reference database comprising a curated
359 protein set from 11 grass species, the Morex V1 protein sequences were on average shorter
360 than their V2 counterparts as indicated by a lower alignment coverage. An analysis of
361 sequence gaps in the intergenic space surrounding genes revealed that 90 % of V2, but only
362 60 % of V1, genes models do not have any "N" bases in their 1-kb flanking regions in the
363 respective sequence assemblies (**Figure S4**). Thus, the Morex V2 gene annotation represents
364 more complete gene models and more regulatory regions around genes compared to the V1
365 annotation. In conclusion, the TRITEX assembly of Morex constitutes a greatly improved
366 barley reference genome and will serve as an important community resource.
367

368 **Discussion**

369

370 We have developed an open-source pipeline for chromosome-scale sequence assemblies of
371 wheat and barley, and validated its performance by comparison to complementary
372 sequence and mapping resources available for the two species. We believe the main
373 application of TRITEX will be in (i) cereal pan-genomics (i.e. assembling genome sequences
374 for representative genotypes, (ii) phylogenomics (i.e. assembling crop-wild relatives in the
375 Triticeae), and (iii) gene isolation (assisting map-based cloning projects) in the immediate
376 future.

377 First, in a pan-genomics scenario it is desirable to achieve chromosome-scale sequences of a
378 (few) dozen genotypes representative of major germplasm groups [23]. An open-source
379 pipeline provides the cereal genomics community with a cost-effective platform to generate
380 comparable genome sequences that are amendable to further improvement and
381 refinement. The up-front cost of purchasing hardware (or leasing cloud computing) and (self-)
382 educating researchers in assembly methodology is justified if many assemblies are done. As

383 service fees for assembly may be as high as the expenses for data generation, academic
384 researchers can double the number accessions included in a pan-genomics project if they
385 perform sequence assembly on their own. Alternatives on-site computing infrastructures are
386 national computing infrastructures such as CyVerse [43], de.NBI [44] or SNIC [45].
387 Second, we anticipate that TRITEX will work well in any diploid or allopolyploid inbreeding
388 Triticeae species. In the Triticeae, important donors of biotic stress resistance loci such as
389 *Ae. sharonensis* [46] or *Ae. longissima* [47] should be amenable to TRITEX assembly.
390 Likewise, our pipeline should be applicable to rye (*Secale cereale*), a minor cereal crop with
391 great importance in East and Central Europe. Although rye is a highly heterozygous,
392 outcrossing species, inbred lines are frequently used by breeders and genomic researchers
393 [48, 49]. TRITEX is likely to work well in species with large and allopolyploid genomes outside
394 the Triticeae tribe such as maize and oats. For maize at least, high-quality sequence
395 assemblies have been constructed with a commercial assembly algorithm [50-52]. However,
396 we must caution users that TRITEX yields assemblies of much lower contiguity and genome
397 representation if closely related haplotypes resident in the same nucleus have to be resolved
398 (Bruno Studer, Martin Mascher; unpublished results). Therefore, we encourage researchers
399 aiming at assembling the genomes of heterozygous, autoploid or dikaryotic species to use
400 long-read sequencing.
401 Third, Thind et al. [53] recently used chromosomal genomics to assist a gene isolation
402 project. They constructed a megabase-scale sequence scaffold of wheat chromosome 2D of
403 cultivar CH Campala harboring flanking markers of a leaf rust resistance locus to isolate a
404 candidate gene, which was absent from the Chinese Spring reference. In cases, where flow-
405 sorting is not possible, the same purpose (albeit at a higher cost) may be served by TRITEX
406 whole-genome assemblies of the parents of a mapping population or near-isogenic lines
407 carrying mutant introgressions. De novo sequence assembly may be of particular relevance
408 to understanding the molecular basis of plant performance in crop-wild introgression lines
409 derived from wide crosses harboring introgressed segments highly divergent from the
410 reference sequence of the domesticate. For example, these might be pre-breeding material
411 with improved disease resistance, but suffering from linkage drag [54], or released wheat
412 cultivars with alien introgressions conferring superior agronomic performance [55].
413 The modular layout of our pipeline lends itself to improvement, replacement or
414 simplification of its components. Compared to DeNovoMagic, TRITEX achieves a lower
415 contiguity at the scaffold level and has a higher proportion of internal gaps (**Tables 3, 4**).
416 Frequent gaps and breaks in repetitive sequence are inherent to short-read assemblies. In
417 fact, long-read assemblies with *contig* N50s exceeding *scaffold* N50s of short-read
418 assemblies have been obtained in other plant and animal species [56-58]. Thus, we propose
419 to improve our Illumina-based scaffolding and gap-filling methodology by integrating long-
420 read sequencing into TRITEX in the future. This can be accomplished either by replacing
421 contigging and mate-pair scaffolding entirely with long-read assembly – contingent on the
422 feasibility of obtaining megabase-scale contig N50s in the Triticeae. Alternatively, contig
423 assembly with PE450 reads may be maintained, but long-read sequences could be used for
424 scaffolding and closing gaps. Depending on their accuracy and relative cost- and time-
425 effectiveness, both approaches may be valid for different applications. Long-read
426 sequencing in the Triticeae may adopt the recently developed circular consensus method of
427 Wenger et al. [59] or improved Nanopore sequencing to obtain highly accurate long-reads.
428 These will likely be crucial to resolve homeologs in polyploid wheat where genic sequence
429 divergence between subgenomes is lower than the error-rate of uncorrected long reads.

430 Our methods for pseudomolecule construction evolved from scripts used for Hi-C mapping
431 of BAC-based sequence scaffolds of barley [3] and whole-genome shotgun assemblies of
432 wheat [4, 17]. They can correct, order and orient along the chromosomes sequence scaffolds
433 of sufficient contiguity and genome representation produced by any sequencing and
434 assembly strategy. We anticipate that even the best long-read assemblies will not be error-
435 free and yield chromosomal contigs without the use complementary linkage information
436 Thus, our methods for assembly correction and super-scaffolding based on linked-read and
437 Hi-C will likely survive the transition to long-reads for contig assembly.
438 For some research purposes, chromosomal sequences may not be required. If a narrow
439 target interval has been defined in a map-based cloning project, PE450 and MP9 reads may
440 suffice to obtain a single sequence scaffold harboring flanking markers at both sides. In this
441 case, Hi-C and even 10X sequencing can be forgone for faster and cheaper assembly, but at
442 the expense of sequence contiguity.

443

444 **Methods**

445

446 *High molecular weight DNA extraction*

447

448 High molecular weight (HMW) DNA depleted for plastidal genomes were prepared from
449 fresh leaves of one-week old seedlings of 'Morex' using a large-scale phenol:chloroform
450 extraction [17]. In short, the protocol involves isolation of nuclei from fresh leaf material,
451 then the nuclei are treated with proteinase-K, and phenol-chloroform extraction removes
452 protein contamination. Then, the HMW DNA was spooled out of the solution using sodium
453 acetate and ethanol precipitation. The extracted DNA was used for preparation of PCR-free
454 paired-end libraries, mate-pair libraries with specific insert sizes and 10X Chromium libraries.

455

456 *Library preparation and sequencing*

457

458 PCR-free paired-end libraries with 400 – 500 bp insert sizes (PE450) for barley cv. Morex
459 were prepared using a custom protocol using the Illumina Truseq PCR-free library
460 preparation kit. The protocol starts with fragmentation of HMW DNA by ultrasound (Covaris
461 S220, Duty Factor 8%, Peak Incident Power 160, Cycles Per Burst 200, Time 60 seconds)
462 followed by BluePippin size selection on a 1.5% cassette with tight 470bp setting. Then, the
463 size-selected DNA was used as input material for Truseq DNA PCR-free library preparation
464 without the SPB bead-based size selection. The prepared libraries were quantified using the
465 KAPA library quantification kit. Sequencing of the PE450 libraries was done on the
466 HiSeq2500 system in Rapid Run mode (2x266 bp reads). The Morex PE800 paired-end library
467 (insert size range: 700 – 800 kb) as well as MP3 (insert size range: 2-4 kb), MP6 (5-7 kb) and
468 MP9 (8-10 kb) mate-pair libraries were constructed and sequenced (2x150 bp reads) at the
469 University of Illinois Roy. J Carver Biotechnology Center.

470 To prepare 10X genomics libraries, genomic DNA (gDNA) was quantified by fluorometry
471 (Qubit 2.0). Small fragments (< 40 kb) were removed from ~2 µg of gDNA using pulsed-field
472 electrophoresis on a Blue Pippin instrument (Sage Science, <http://www.sagescience.com>)
473 following the high-pass protocol. Recovered HMW DNA was evaluated for integrity and size
474 (> 48.5 kb) on a Tapestation 2200 (Agilent, <https://www.agilent.com>), and quantified (Qubit
475 2.0, <https://www.thermofisher.com/de/en/home/industrial/spectroscopy-elemental-isotope-analysis/molecular-spectroscopy/fluorometers/qubit.html>). Library preparation
476 followed the 10X Genome Chromium library protocol v1 (10X Genomics,
477

478 <https://www.10xgenomics.com>). Four individual libraries were prepared and uniquely
479 indexed for multiplexing, and quantified by qPCR (Kapa Biosystems). Libraries were
480 normalized and pooled for sequencing on two lanes of an Illumina HiSeq2500 instrument in
481 PE125 mode using v4 chemistry for high output. Pooled libraries were de-multiplexed with
482 Supernova (10X Genomics) and FASTQ files generated with Longranger (10X Genomics).
483

484 *Preprocessing of paired-end and mate-pair reads*

485

486 Overlapping single reads of the PE450 libraries were merged with PEAR [25] (Zavitan), or
487 with BBMerge [26] (Chinese Spring, Morex) using the ‘maxloose’ strictness setting. Error-
488 correction of merged PE450 reads was done with BFC [27] in two passes. After the first BFC
489 pass (correction), reads containing singleton k-mers were trimmed using a k-mer size of 61.
490 Illumina adapters were trimmed from the PE800 read using Cutadapt [60]. Nextera junction
491 adapters and short-insert contaminants were removed from mate-pair reads using NxTrim
492 [61]. Trimmed PE800 and mate-pair reads were corrected with BFC [27] using the hash table
493 of k-mer counts generated from the PE450 reads.

494

495 *Unitig assembly*

496

497 Minia3 ([30], <https://github.com/GATB/minia>) was used to assemble corrected and trimmed
498 PE450 reads into unitigs. The Minia3 source was assembled to enable k-mer size up to 512
499 as described in the Minia3 manual. The parameters “-no-bulge-removal -no-tip-removal -no-
500 ec-removal” were used to disable the resolution of ambiguous paths. Iterative Minia3 runs
501 with increasing k-mer sizes (100, 200, 300, 350, 400, 450, 500) were used as proposed in the
502 GATB Minia pipeline (<https://github.com/GATB/gatb-minia-pipeline>). In the first iteration,
503 the input reads were assembled using a k-mer size of 100. In the subsequent runs, the input
504 reads as well as the assembly of the previous iteration were used as input for the assembler.
505

506

507 *Scaffolding and gap-closing*

508

509 Error-corrected PE800, MP3, MP6 and MP9 reads were used for scaffolding with
510 SOAPDenovo2 [62]. The “fusion” module (<https://github.com/aquaskyline/SOAPdenovo2>)
511 was used to prepare the Minia3 unitigs for use with SOAPDenovo2. The “map” was used to
512 align reads to the unitigs. A range of parameters for “pair_num_cutoff” (minimum of read
513 pairs linking two sequences) for each library were tested with the “scaff” module with gap-
514 filling disabled, and the “pair_num_cutoff” value resulting in the best N50 was chosen. Once
515 the best thresholds had been determined, the “scaff” module was run with gap-filling
516 enabled (parameter -F).

517 GapCloser (<https://sourceforge.net/projects/soapdenovo2/files/GapCloser/src/r6/>) was
518 used to fill internal gaps in scaffolds using the error-corrected PE450 reads.

519

520 *Alignment of 10X Chromium reads and molecule calling*

521

522 Before alignment, the FASTQ files of read 1 and read 2 were interleaved with Seqtk
523 (<https://github.com/lh3/seqtk>). Then, the first 23 nt of read 1 were removed and the
524 instrument name in the Illumina read identifier was replaced by the 10X barcode (the first 16
525 nt of read 1). Illumina adapters were trimmed using cutadapt [60] using the adapter
sequence AGATCGGAAGAGC. Reads shorter than 30 bp after trimming were discarded.

526 Trimmed reads were aligned to the assembly after the GapCloser step using Minimap2 [36].
527 Alignment records were converted to the Binary Sequence Alignment/Map (BAM) Format
528 with SAMtools [63]. BAM files were sorted twice with Novosort
529 (<http://www.novocraft.com/products/novosort/>). First, reads were sorted by alignment
530 positions and duplicated read pairs were flagged. Then, reads were sorted by name to group
531 read pairs with identical barcodes together. After sorting, BAM files were converted into
532 BEDPE format using BEDTools [64]. Duplicated and supplementary alignments were ignored.
533 Only read pairs with a mapping quality ≥ 20 were retained. Read pairs with an estimated
534 insert size above 800 bp were discarded. Read pairs were written into a table with four
535 columns (chromosome, start, end, barcode), which was sorted by barcode and alignment
536 position using GNU sort. Read pairs having the same barcode and mapping within 500 kb of
537 each other were assigned to the same molecule. A table recording the barcodes as well as
538 the start and end points of each molecule was exported as a text file. Molecules shorter than
539 1 kb were discarded.

540

541 *10X super-scaffolding*

542

543 A graph structure is constructed in which nodes are scaffolds and edges are drawn between
544 if a sufficient number of 10X links meet certain criteria. Only molecules mapping within 100
545 kb of the scaffold ends are considered. Edges between scaffolds are accepted only if they are
546 supported by molecules from more than one Chromium library. In the initial graph, only
547 molecules connecting scaffolds anchored by POPSEQ to the same chromosome within 5 cM
548 of each other are allowed. A minimum spanning tree is computed with functionalities of the
549 R package igraph [65]. Subsequently, heuristics are applied to resolve branches to obtain
550 subgraphs that are paths. Heuristics include (i) the removal of tips (nodes of rank one), (ii)
551 nodes corresponding to small (< 10 kb) scaffolds, and (iii) cutting the tree at branch points by
552 removing edges. These subgraphs are the initial super-scaffolds and the order of scaffolds in
553 them is determined by the (well-defined) path traversing each subgraph. The orientation of
554 a scaffold S within a super-scaffold X is determined by calculating the mean position of
555 molecules linking S to other scaffolds in X up to five bins upstream (to the left) or
556 downstream (to the right) of S. If the average position of downstream links is larger than
557 that of the upstream links, the orientation of S is “forward”, and “reverse” otherwise. Super-
558 scaffolds are assigned to POPSEQ genetic positions by lifting positional information from
559 their constituent scaffolds (see below) and computing a consensus. Super-scaffold
560 construction is repeated with different thresholds for the minimum number of read pairs to
561 assign molecules to scaffold (2 to 10) and the minimum number of molecules required to an
562 accept edges between scaffold pairs (2 to 10) and the assembly with the highest N50 is
563 selected for further steps.

564

565 *Hi-C map construction*

566

567 Scaffolds after the GapCloser step were digested *in silico* with EMBOSS restrict [66]. Reads
568 were aligned to the scaffolds and assigned to restriction fragments as described by Beier et
569 al. [34]. In contrast to Beier et al., we used Minimap2 [36] instead of BWA-MEM [67] for
570 read alignment. Scaffolds were assigned to chromosomes using the POPSEQ genetic maps of
571 wheat and barley [12, 13] as described by Avni et al. [17]. POPSEQ marker sequences (the
572 scaffolds of synthetic wheat W7984 assembled by Chapman et al. [13] or the WGS contigs of
573 the International Barley Sequencing Consortium (2012) [39]) were aligned to the scaffolds

574 using Minimap2 [36]. POPSEQ positional information and Hi-C links were lifted from
575 scaffolds to super-scaffolds. Super-scaffolds were ordered and oriented as described by
576 Beier et al. [34]. Intra-chromosomal Hi-C matrices were normalized with HiCNorm [68] and
577 visually inspected in a locally installed R Shiny app. The code for the Shiny app is provided in
578 the Bitbucket repository.

579

580 *Discovery and correction of mis-assemblies*

581

582 We follow the approach of Putnam et al. [69] and Ghurye et al. [33] by detecting sequence
583 mis-joins made during the scaffold stage by inspecting the physical coverage with either 10X
584 molecules or Hi-C links. To find breakpoints based on 10X (Hi-C) data, scaffolds were divided
585 into 200 bp (1 kb) bins and the number of molecules (Hi-C links) spanning each bin was
586 calculated. Links counts were normalized by distance from the scaffolds ends. Drops in 10X
587 coverage below one eighth of the genome-wide average were considered as breakpoints.
588 The minimum distance between two breakpoints was 50 kb. After breaking chimeras,
589 POPSEQ marker positions, 10X molecule boundaries and Hi-C links were lifted to the
590 corrected assemblies. This procedure was repeated until no breakpoints were detected.
591 Drops in Hi-C coverage below one sixteenth of the genome-wide average were considered as
592 potential breakpoints and diagnostic plots summarizing POPSEQ marker information as well
593 as Hi-C coverage along scaffolds were visually inspected. If necessary, breakpoint
594 coordinates were adjusted manually.

595

596 *Dovetail assembly*

597

598 Chicago libraries were prepared from leaves of barley cv. Morex by Dovetail Inc. as described
599 by Putnam et al. [41]. The HiRise algorithm was used to scaffold the non-redundant BAC-
600 based sequence contigs assembled by Mascher et al. [3] (accessible from
601 <http://dx.doi.org/10.5447/IPK/2016/30>).

602

603 *Optical map alignment*

604

605 The genome-wide optical map of barley cv. Morex [3] was retrieved from
606 <http://dx.doi.org/10.5447/IPK/2016/31> and aligned to the TRITEX super-scaffolds using
607 Bionano RefAligner (<https://bionanogenomics.com>). Custom scripts were used for importing
608 alignments into R and visualization
609 (<https://bitbucket.org/tritexassembly/tritexassembly.bitbucket.io/src/master/miscellaneous/bionano.R>).
610

611

612 *Assembly-to-assembly alignment*

613

614 Recent versions of Minimap2 ([36], <https://github.com/lh3/minimap2>) were used for
615 assembly-to-assembly alignment. Alignment records were written to PAF format and
616 imported into R for visualization and calculation of summary statistics.

617

618 *Transcript alignment*

619

620 Transcript datasets were aligned with GMAP [70] version 2018-07-04 to genomic references.
621 Alignment records were written to GFF files, from which coverage and alignment identity for
622 mRNA alignments were extracted.

623

624 *Barley gene annotation*

625

626 Our annotation pipeline combines three types of evidence for structural gene annotation in
627 plants: protein homology, expression data and *ab initio* prediction. For homology-based
628 annotation, we combined available Triticeae protein sequences obtained from UniProt
629 (05/10/2016). These protein sequences were mapped to the nucleotide sequence of the
630 Morex V2 pseudomolecules using the splice-aware alignment software GenomeThreader
631 [71] (version 1.7.1; arguments -startcodon -finalstopcodon -species rice -gcmincov 70 -
632 prseedlength 7 -prhdist 4). Full-length cDNA [72] and IsoSeq [3] nucleotide sequences were
633 aligned to the Morex V2 pseudomolecules using GMAP [70] (version 2018-07-04, standard
634 parameters). Illumina RNA-seq datasets were first mapped using Hisat2 [73] (version 2.0.4,
635 parameter --dta) and subsequently assembled into transcript sequences by Stringtie [74]
636 (version 1.2.3, parameters -m 150 -t 0.3. Full-length cDNA, IsoSeq sequences and RNASeq
637 datasets are described in [3]. All transcripts from flcDNA, IsoSeq and RNASeq were combined
638 using Cuffcompare [75] (version 2.2.1) and subsequently merged with Stringtie (version
639 1.2.3, parameters --merge -m 150) to remove fragments and redundant structures. Next, we
640 used Transdecoder (version 3.0.0, <https://github.com/TransDecoder>) to find potential open
641 reading frames and to predict protein sequences. We used BLASTP [76] (ncbi-blast-2.3.0+,
642 parameters -max_target_seqs 1 -evalue 1e-05) to compare potential protein sequences with
643 a trusted set of reference proteins (Uniprot Magnoliophyta, reviewed/Swissprot,
644 downloaded on 3 Aug 2016) and used hmmscan [77] (version 3.1b2) to identify conserved
645 protein family domains for all potential proteins. BLAST and hmmscan results were fed back
646 into Transdecoder-predict to select the best translations per transcript sequence.

647 An independent *ab initio* annotation using Augustus [78] (version 3.3.2) was carried out to
648 further improve structural gene annotation. To minimize over-prediction, hint files using the
649 above mentioned IsoSeq, flcDNA, RNASeq, protein evidences and TE predictions were
650 generated. The wheat model was used for prediction.

651 All structural gene annotations were joined by feeding them into EVidenceModeler [79] and
652 weights were adjusted according to the input source. To refine gene models, we also
653 incorporated the Barley reference transcript database (BaRT) as an additional source. All
654 BaRT transcripts were aligned to the new Morex V2 assembly using GMAP (version 2018-07-
655 04) and output was converted into GFF format and subsequently fed into EVidenceModeler.
656 Finally, redundant protein sequences were removed to form a single non-redundant
657 candidate dataset. To categorize candidates into complete and valid genes, non-coding
658 transcripts, pseudogenes and transposable elements, we applied a confidence classification
659 protocol. Candidate protein sequences were compared against the following three manually
660 curated databases using BLAST: first, PTREP, a database of hypothetical proteins that
661 contains deduced amino acid sequences in which, in many cases, frameshifts have been
662 removed, which is useful for the identification of divergent TEs having no significant
663 similarity at the DNA level; second, UniPoa, a database comprised of annotated Poaceae
664 proteins; third, UniMag, a database of validated magnoliophyta proteins. UniPoa and
665 UniMag protein sequences were downloaded from Uniprot and further filtered for complete
666 sequences with start and stop codons. Best hits were selected for each predicted protein to
667 each of the three databases. Only hits with an E-value below 10^{-10} were considered.

668 Furthermore, only hits with subject coverage (for protein references) or query coverage
669 (transposon database) above 75% were considered significant and protein sequences were
670 further classified using the following confidence: a high confidence (HC) protein sequence is
671 complete and has a subject and query coverage above the threshold in the UniMag database
672 (HC1) or no blast hit in UniMag but in UniPoa and not TREP (HC2); a low confidence (LC)
673 protein sequence is not complete and has a hit in the UniMag or UniPoa database but not in
674 TREP (LC1), or no hit in UniMag and UniPoa and TREP but the protein sequence is complete.
675 The tag REP was assigned for protein sequences not in UniMag and complete but with hits in
676 TREP.
677 Functional annotation of predicted protein sequences was done using the AHRD pipeline
678 (<https://github.com/groupschoof/AHRD>). Completeness of the predicted gene space was
679 measured with BUSCO [42] (version 3.02, orthodb9).
680

681 *Analysis of 5' and 3' flanking regions of gene models*

682
683 5' and 3' flanking nucleotide sequences of increasing lengths in the range from 1 kb to 10 kb
684 upstream and downstream of predicted gene models were extracted and sequences
685 containing N were discarded. The remaining N-free sequences were counted and plotted as
686 a percentage of the total number of predicted gene models.
687

688 *Repeat annotation*

689
690 Transposons where detected and classified by an homology search against the
691 REdat_9.7_Triticeae subset of the PGSB transposon library [80] using vmatch
692 (<http://www.vmatch.de>) using following parameter settings: identity >= 70%, minimal hit
693 length 75 bp, seed length 12 bp (exact command line: -d -p -l 75 -identity 70 -seedlength 12 -
694 exdrop 5). The vmatch output was filtered for redundant hits via a priority-based approach,
695 which assigns higher scoring matches first and either shortens (< 90% coverage and >= 50bp
696 rest length) or removes lower scoring overlaps, leading to an overlap free annotation.
697 Full-length LTR retrotransposons where identified with LTRharvest [81] using the following
698 parameters: "overlaps best -seed 30 -minlenltr 100 -maxlenltr 2000 -mindistltr 3000 -
699 maxdistltr 25000 -similar 85 -mintsd 4 -maxtsd 20 -motif tgca -motifmis 1 -vic 60 -xdrop 5 -
700 mat 2 -mis -2 -ins -3 -del -3". All candidates from the LTRharvest output were subsequently
701 annotated for PfamA domains using hmmer3 [82] and stringently filtered for false positives
702 by several criteria, the main ones being a lack of at least one typical retrotransposon domain
703 [e.g. reverse transcriptase (RT), RNase H (RH), integrase (INT), protease (PR), etc.]) and a
704 tandem repeat content > 25%. The inner domain order served as a criterion for the
705 classification into the Gypsy (RT-RH-INT) or Copia (INT-RT-RH) superfamily abbreviated as
706 RLG and RLC. Elements missing either INT or RT were classified as RLX. The insertion age of
707 each full-length LTR retrotransposon was estimated based on the accumulated divergence
708 between its 5' and 3' long terminal repeats and a mutation rate of 1.3×10^{-8} [83].
709 Tandem repeats where identified with the TandemRepeatFinder [84] using default
710 parameters and subjected to an overlap removal as described above, prioritizing longer and
711 higher scoring elements. K-mer frequencies were calculated with Tallymer [85].
712

713 *Representation of selected TE families*

714

715 We identified full-length copies belonging to single TE families in the assemblies of Chinese
716 Spring and Morex. Our pipeline uses BLASTN [76] to search for long terminal repeats (LTRs)
717 that occur at a user-defined distance range in the same orientation. For RLC_BARE1 and
718 RLC_Angela elements, the two LTRs had to be found within a range of 7,800-9,300 bp (a
719 consensus RLC_BARE1 sequence has a length of approximately 8,700 bp), while a range from
720 6,000-10,000 bp was allowed for RLG_Sabrina elements. Multiple different LTR consensus
721 sequences were used for the searches in order to cover the intra-family diversity. Five LTR
722 consensus sequences each were used for RLC_BARE1 and RLG_Sabrina elements, while 18
723 LTR consensus sequences were used for RLC_Angela elements (to cover the much wider
724 diversity of this family in the three wheat subgenomes). The LTR consensus sequences from
725 the same families are 73-92% identical to each other, reflecting the considerable intra-family
726 diversity.

727 For the current analysis, full-length copies of RLC_BARE1 and their wheat homologs
728 RLC_Angela elements were extracted because these are the most abundant families in
729 barley and wheat genomes, respectively. RLG_Sabrina was chosen because preliminary
730 analyses showed that this TE family has not been active in wheat for a long time and thus is
731 represented mostly by old copies.

732 To validate the extracted TE populations, the size range of all isolated copies as well as the
733 number of copies that are flanked by a target site duplication (TSD) were determined. A TSD
734 is accepted if it contains at least 3 matches between 5' and 3' TSD (e.g. ATGCG and ACGAG).
735 This low stringency was applied because our previous study showed that TSD generation is
736 error-prone, and thus multiple mismatches can be expected [86]. In a survey, 80-90% of all
737 isolated full-length elements were flanked by a TSD.

738 Our pipeline also extracts so-called “solo-LTRs”. These are products of intra-element
739 recombination that results in the loss of the internal domain and the generation of a
740 chimeric solo-LTR sequence. Solo-LTRs were used as a metric of how well short repetitive
741 sequences are assembled.

742

743 *Data availability*

744

745 Paired-end and mate-pair data for Zavitan [17] and Chinese Spring [4] were retrieved from
746 EMBL ENA (accession numbers: PRJEB31422 and SRP114784). Paired-end, mate-pair, 10X
747 and Chicago data generated for Morex were deposited under ENA project ID PRJEB31444.
748 Hi-C data for barley cv. Morex [3] are available under ENA accession PRJEB14169. Sequence
749 assemblies generated in the present study are accessible under the following Digital Object
750 Identifiers (DOIs) in the Plant Genomics & Phenomics Research Data Repository [87]:
751 doi:10.5447/IPK/2019/6 (wheat assemblies); doi:10.5447/IPK/2019/8 (barley Morex V2
752 assembly); doi: 10.5447/IPK/2019/7 (barley Dovetail assembly). DOIs were registered with
753 e!DAL [88].

754

755 *Access to source code, documentation and software versions*

756

757 Z shell scripts were used to call assembly and alignment software. GNU Parallel [89] was
758 used for parallel computing. Scaffolding with 10X and Hi-C data was implemented in GNU
759 AWK (<https://www.gnu.org/s/gawk/manual/gawk.html>) and R [31] scripts. R code relies
760 heavily on the data.table package (<https://cran.r-project.org/package=data.table>) for in-
761 memory data management and analysis. A step-by-step usage guide was prepared using the
762 AsciiDoc markup language (<https://asciidoc.org/docs/what-is-asciidoc/>) is available from

763 <https://nomagicassembly.bitbucket.io>. A list of software versions known to work with
764 TRITEX is included in the usage guide. Source code is hosted in a public Bitbucket repository
765 (<https://bitbucket.org/nomagicassembly/nomagicassembly.bitbucket.io>). Assemblies were
766 run on compute servers at IPK Gatersleben. The most powerful of these has 72 physical
767 cores (Intel Xeon E7-8890 v3) and 2 TB of main memory. We had access to 100 TB of hard
768 disk space and 22 TB of SSD storage.

769

770 **Author Contributions**

771

772 M.M. and N.S. conceived the study. S.P. and A.H. performed library preparation and
773 sequencing. M.M. designed the computational workflow. C.M. and M.M. performed
774 assembly. T.W. and H.G. analyzed transposable elements. T.L., H.G., M.S. and K.F.X.M.
775 performed genome annotation. J.E. and C.P. constructed 10X libraries. U.S. supervised IT
776 administration. I.B., C.L., M.M., K.F.X.M, G.J.M, A.H.S, N.S. and R.W. contributed the Dovetail
777 assembly. C.M. and M.M. wrote the paper with input from all co-authors.

778

779 **Acknowledgements**

780

781 This research was supported by grants from the German Federal Ministry of Education and
782 Research to N.S., M.M., U.S., M.S. and K.F.X.M ('SHAPE', FKZ 031B0190), to U.S. and K.F.X.M
783 ('De.NBI', FKZ 031A536) and from the German Federal Ministry of Food and Agriculture to
784 K.F.X.M (grant 2819103915, 'Wheatseq'). Support for 10X sequencing was provided by a
785 research grant from Genome Canada and Genome Prairie (to C.P. and J.E). Tim Close
786 (University of California, Riverside) contributed funds from Hatch Project CA-R-BPS-5306-H
787 to the Dovetail assembly. We are indebted to Rayan Chikhi for pointing us to the multi k-mer
788 approach. We are grateful to Manuela Knauft, Ines Walde and Susanne König for technical
789 assistance. We thank Anne Fiebig for handling data submission and Jens Bauernfeind,
790 Thomas Münch and Heiko Miehe for IT administration. We thank Johannes Heilmann for
791 introducing us to AsciiDoc, and Sara Giulia Milner, Kevin Koh, Liangliang Gao, Juan Gutierrez
792 Gonzalez, Burkhard Steuernagel, Kumar Gaurav and Raz Avni for feedback on previous
793 versions of the workflow.

794

795 **Tables**

796

797 **Table 1: Input datasets for TRITEX.**

798

Name	Library type (number ¹)	Insert size	Read length	Coverage ²
PE450	PCR-free paired-end (2)	400-470 bp	2x250 bp	70x
PE800	PCR-free paired-end (2)	700-800 bp	2x150 bp	30x
MP3	Nextera mate-pair (2)	2-4 kb	2x150 bp	30x
MP6	Nextera mate-pair (2)	5-7 kb	2x150 bp	30x
MP9	Nextera mate-pair (2)	8-10 kb	2x150 bp	30x
10X	10X Chromium (2)		2x150 bp	30x
Hi-C	TCC [90] or in-situ Hi-C [91] (1)		2x100 bp	200 – 400 million read pairs

799 ¹Number of independent libraries to be prepared.

800 ²Haploid genome coverage for paired-end, mate-pair and 10X libraries. As Hi-C analysis is count-based, read numbers are more relevant than
801 sequence amount.

802

803

Table 2: Overview of the TRITEX pipeline.

804

Step ¹	Software	Input	Output
1 Read merging	BBMerge [26]	PE450 read pairs	Merged PE450 reads
2 PE450 error-correction	BFC [27]	Merged PE450 reads	Corrected PE450 reads Hash table of k-mer counts
3.1 Unitig assembly	Minia3 [29, 30]	Corrected PE450 reads	Unitigs
3.2 Error-correction of PE800 and MP reads	BFC [27] Cutadapt [60], NxTrim [61]	PE800, MP3, MP6, MP9 reads Hash table of k-mer count (step 2)	Corrected PE800, MP3, MP6 and MP9 reads
4 Scaffolding	SOAPDenovo2 [62]	Unitigs Corrected PE800, MP3, MP6, MP9 reads	Scaffolds
5 Gap-filling	Gapcloser [62]	Scaffolds Corrected PE450 reads	Scaffolds after gap-filling
6.1 Alignment of 10X reads	Minimap2 [36], cutadapt [60], SAMtools [63], BEDtools [64], custom scripts	Scaffolds after gap-filling 10X reads	10X alignment records
6.2 Alignment of Hi-C reads	As in 6.2 EMBOSS [66]	Scaffolds after gap-filling Hi-C reads	Hi-C alignment records
6.3 Alignment of genetic markers	Minimap2 [36]	Scaffolds after gap-filling Marker sequences	Marker alignment records
7 Pseudomolecule construction	Custom R scripts	Scaffolds after gap-filling 10X alignment records Hi-C alignment records Marker alignment records	Pseudomolecules Hi-C contact maps

805

¹Steps with identical leading digits can be run in parallel.

806

807

808

809

810

811

Table 3: Assembly statistics for Zavitan and Chinese Spring.

	Zavitan		Chinese Spring	
	TRITEX	Avni et al. [8]	TRITEX	IWGSC [4]
Unitig assembly size	10.8 Gb		15.1 Gb	
Unitig N50	21.7 kb		21.4 kb	
Unitig N90	1.5 kb		1.7 kb	
Assembled sequence in contigs >= 1 kb	10.0 Gb		14.0 Gb	
Assembled sequence in contigs >= 10 kb	7.8 Gb		10.8 Gb	
Scaffold assembly size	11.1 Gb	10.5 Gb	15.7 Gb	14.5 Gb
Scaffold N50	1.3 Mb	7.0 Mb	2.3 Mb	7.0 Mb
Scaffold N90	97 kb	1.2 Mb	281 kb	1.2 Mb
Assembled sequence in scaffolds >= 1 kb	10.4 Gb	10.5 Gb	14.8 Gb	14.5 Gb
Assembled sequence in scaffolds >= 1 Mb	6.7 Gb	9.6 Gb	11.9 Gb	13.4 Gb
Unfilled internal gaps	209 Mb (1.9 %)	171 Mb (1.6 %)	476 Mb (3.0 %)	262 Mb (1.8 %)

812

813

Table 4: Comparison of different assemblies of barley cv. Morex

	BAC-by-BAC		TRITEX	TRITEX
	Morex V1 [3]	Dovetail	Morex V2	MP9 only
Scaffold assembly size	4.79 Gb		4.65 Gb	4.6 Gb
Scaffold N50	79 kb		3.4 Mb	2.6 Mb
Scaffold N90	4.4 kb		287 kb	150 kb
Assembled sequence in scaffolds >= 1 kb	4.67 Gb		4.34 Gb	4.32 Gb
Assembled sequence in scaffolds >= 1 Mb	0 bp		3.80 Gb	3.49 Gb
Unfilled internal gaps	216 Mb (4.5 %)		116 Mb (2.5 %)	106 Mb (2.3 %)
Super-scaffold N50	1.9 Mb	1.3 Mb	40.2 Mb	32.6 Mb
Super-scaffold N90	336 kb	7.5 kb	2.0 Mb	1.2 Mb
Size of pseudomolecules	4.58 Gb		4.26 Gb	4.20 Gb
Size of unanchored sequences (chrUn)	246 Mb		83 Mb ²	111 Mb ²
Proportion of complete full-length cDNAs¹	81.8 %	84.1 %	89.8 %	90.4 %

814 ¹Proportion of 28,622 full-length cDNAs of barley cv. Haruna Nijo [72] aligned with >= 90 % coverage and >= 97 % alignment identity.815 ²Sequences shorter than 1000 kb were not included in chrUn.

816

817

Table 5: Chinese Spring transcript alignment statistics.

818

Transcript dataset	No. of transcripts	Assembly	Proportion of complete transcripts ¹
IWGSC v1.0 transcripts [4]	269,583	TRITEX	96.2 %
		IWGSC [4]	97.0 %
		Clavijo et al. [20]	87.8 %
		Zimin et al. [22]	88.5 %
Full-length cDNAs [37]	6,137	TRITEX	97.1 %
		IWGSC [4]	96.3 %
		Clavijo et al. [20]	91.6 %
		Zimin et al. [22]	85.4 %

819

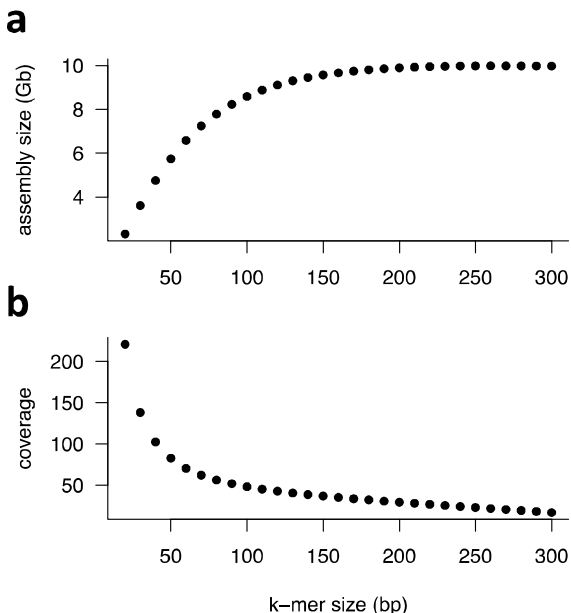
¹ Proportion of transcripts with at least one alignment with $\geq 99\%$ coverage and $\geq 99\%$ identity (for IWGSC transcripts) or with $\geq 90\%$ coverage and $\geq 99\%$ identity (for full-length cDNAs). Alignments were done with GMAP [70].

820

821

822 **Figures**

823

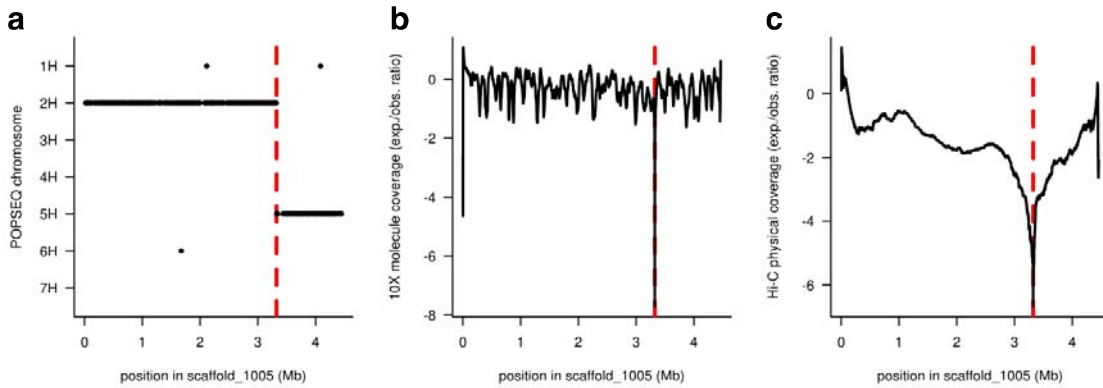


824

825

826 **Figure 1: Estimate of assembly size and k-mer coverage as a function of k-mer size.**
827 Assembly size **(a)** and k-mer coverage **(b)** were estimated from error-corrected PE450 used
828 for Zavitan unitig assembly based on k-mer cardinalities using NtCard [92] and Kmerstream
829 [28].

830

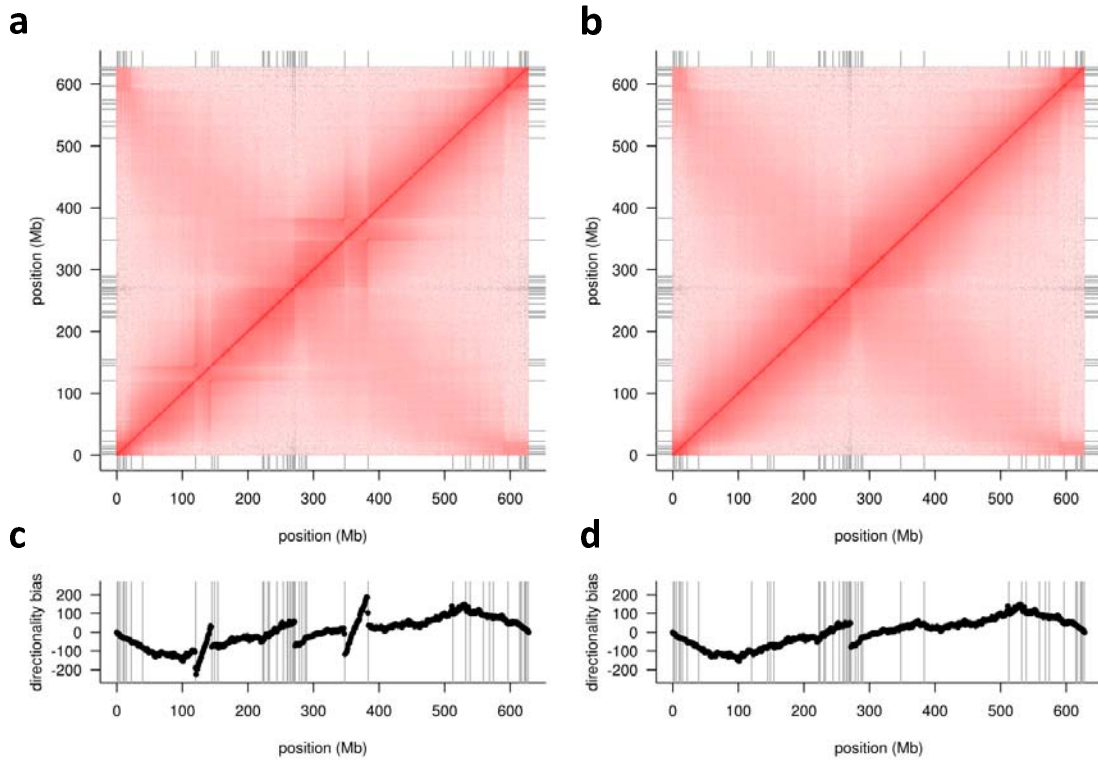


831

832

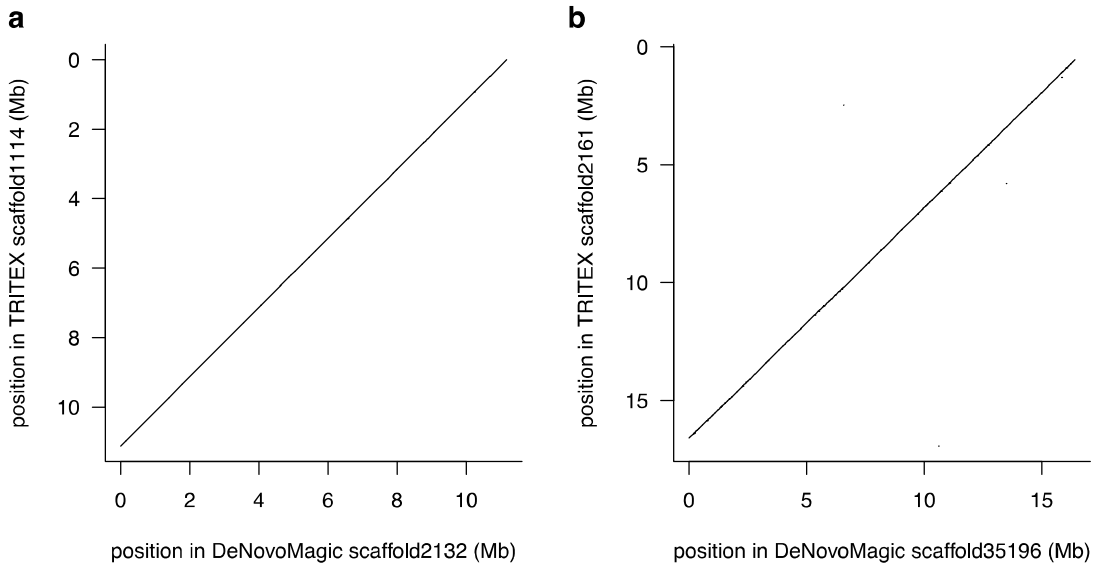
833 **Figure 2: Example of a chimeric scaffold.** The chimeric nature of a sequence scaffold joining
834 two unlinked sequences originating from barley chromosomes 2H and 5H is supported by
835 multiple lines of evidence. **(a)** Genetic chromosome assignments of marker sequences
836 aligned to scaffold_1005. **(b)** 10X molecule coverage. **(c)** Physical Hi-C coverage. Coverage in
837 panels **(b)** and **(c)** was normalized for distance from the scaffold ends and the log2-fold
838 observed vs. expected ratio was plotted. The red, dotted lines mark the breakpoint at 3.32
839 Mb.

840

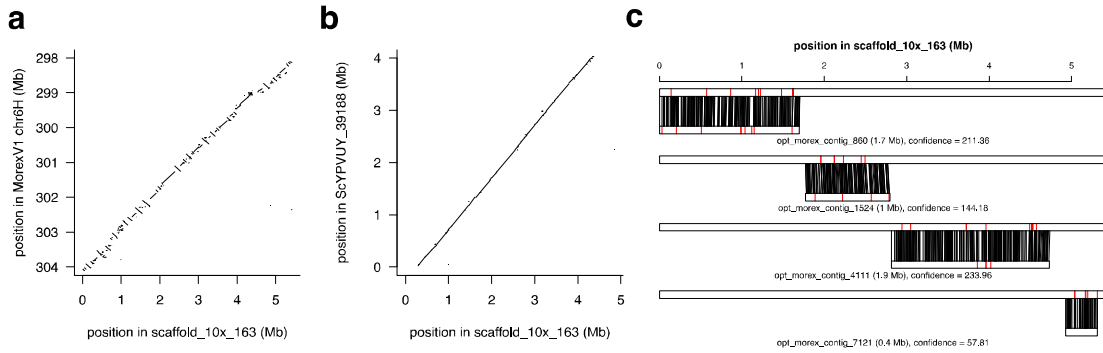


841
842

843 **Figure 3: Example of errors in scaffold orientation.** The top panels show the Hi-C contact
844 matrix for barley chromosome 3H before (a) and after (b) manual correction. The bottom
845 panels show the directionality biases in the Hi-C data as defined by Himmelbach et al. [93]
846 before (c) and after (d) manual correction. Two inverted scaffolds are evident as deviations
847 from the expected Rabl configuration [3] and as diagonals bounded by discontinuities in the
848 directionality biases.
849

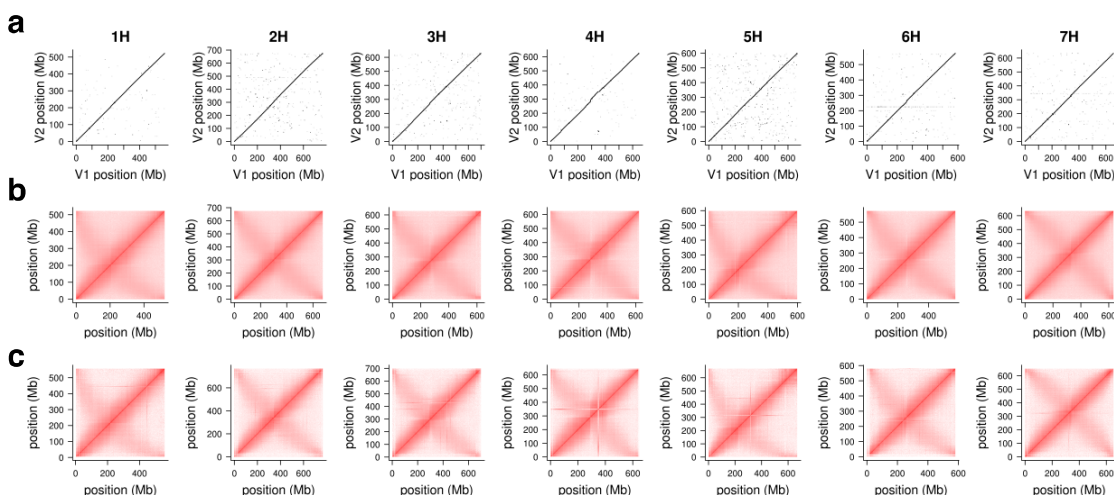


850
851
852 **Figure 4: Collinearity between TRITEX and DeNovoMagic assemblies of wheat.** Dotplots
853 showing the longest alignments between scaffold pairs of the TRITEX and DeNovoMagic
854 assemblies of Zavitan **(a)** and Chinese Spring **(b)**, respectively. Alignments were done with
855 Minimap2 [36].
856



857
858

859 **Figure 5: Morex V2 assembly validated by complementary resources.** Morex
860 scaffold_10x_163 was aligned to the Morex V1 assembly (a), the Dovetail assembly of Morex
861 (b) and the genome-wide optical map of Morex (c). Sequence alignments are shown as dot
862 plots (a, b). Panel (c) shows the alignment of four optical contigs to scaffold_10x_163. Single
863 aligned restriction sites are connected by black lines. Red lines indicate unaligned restriction
864 sites in either the sequence scaffold or the optical contig.
865



866
867

868 **Figure 6: Collinearity of Morex V1 and V2 assemblies. (a)** Dot plots showing the alignments
869 between the chromosomal pseudomolecules of the Morex V1 and V2 assemblies. **(b)** Intra-
870 chromosomal Hi-C contact matrices of the Morex V2 assembly. **(c)** Intra-chromosomal Hi-C
871 contact matrices of the Morex V1 assembly.

872

873 **References**

874

875 1. Schulte D, Close TJ, Graner A, Langridge P, Matsumoto T, Muehlbauer G, Sato K,
876 Schulman AH, Waugh R, Wise RP: **The international barley sequencing consortium—**
877 **at the threshold of efficient access to the barley genome.** *Plant physiology* 2009,
878 **149**:142-147.

879 2. Gill BS, Appels R, Botha-Oberholster AM, Buell CR, Bennetzen JL, Chalhoub B,
880 Chumley F, Dvorak J, Iwanaga M, Keller B, et al: **A workshop report on wheat**
881 **genome sequencing: International Genome Research on Wheat Consortium.**
882 *Genetics* 2004, **168**:1087-1096.

883 3. Mascher M, Gundlach H, Himmelbach A, Beier S, Twardziok SO, Wicker T, Radchuk V,
884 Dockter C, Hedley PE, Russell J, et al: **A chromosome conformation capture ordered**
885 **sequence of the barley genome.** *Nature* 2017, **544**:427-433.

886 4. The International Wheat Genome Sequencing Consortium (IWGSC): **Shifting the**
887 **limits in wheat research and breeding using a fully annotated reference genome.**
888 *Science* 2018, **361**:eaar7191.

889 5. Maccaferri M, Harris NS, Twardziok SO, Pasam RK, Gundlach H, Spannagl M,
890 Ormanbekova D, Lux T, Prade VM, Milner SG, et al: **Durum wheat genome highlights**
891 **past domestication signatures and future improvement targets.** *Nature Genetics*
892 2019.

893 6. Luo MC, Gu YQ, Puiu D, Wang H, Twardziok SO, Deal KR, Huo N, Zhu T, Wang L, Wang
894 Y, et al: **Genome sequence of the progenitor of the wheat D genome *Aegilops***
895 ***tauschii*.** *Nature* 2017, **551**:498-502.

896 7. Ling HQ, Ma B, Shi X, Liu H, Dong L, Sun H, Cao Y, Gao Q, Zheng S, Li Y, et al: **Genome**
897 **sequence of the progenitor of wheat A subgenome *Triticum urartu*.** *Nature* 2018,
898 **557**:424-428.

899 8. Avni R, Nave M, Barad O, Baruch K, Twardziok SO, Gundlach H, Hale I, Mascher M,
900 Spannagl M, Wiebe K: **Wild emmer genome architecture and diversity elucidate**
901 **wheat evolution and domestication.** *Science* 2017, **357**:93-97.

902 9. McPherson JD, Marra M, Hillier L, Waterston RH, Chinwalla A, Wallis J, Sekhon M,
903 Wylie K, Mardis ER, Wilson RK, et al: **A physical map of the human genome.** *Nature*
904 2001, **409**:934-941.

905 10. Beier S, Himmelbach A, Schmutz T, Felder M, Taudien S, Mayer KF, Platzer M, Stein
906 N, Scholz U, Mascher M: **Multiplex sequencing of bacterial artificial chromosomes**
907 **for assembling complex plant genomes.** *Plant biotechnology journal* 2016, **14**:1511-
908 1522.

909 11. Choulet F, Alberti A, Theil S, Glover N, Barbe V, Daron J, Pingault L, Sourdille P,
910 Couloux A, Paux E: **Structural and functional partitioning of bread wheat**
911 **chromosome 3B.** *Science* 2014, **345**:1249721.

912 12. Mascher M, Muehlbauer GJ, Rokhsar DS, Chapman J, Schmutz J, Barry K, Muñoz-
913 Amatriaín M, Close TJ, Wise RP, Schulman AH, et al: **Anchoring and ordering NGS**
914 **contig assemblies by population sequencing (POPSEQ).** *The Plant Journal* 2013,
915 **76**:718-727.

916 13. Chapman JA, Mascher M, Buluc A, Barry K, Georganas E, Session A, Strnadova V,
917 Jenkins J, Sehgal S, Oliker L, et al: **A whole-genome shotgun approach for assembling**
918 **and anchoring the hexaploid bread wheat genome.** *Genome Biol* 2015, **16**:26.

919 14. Burton JN, Adey A, Patwardhan RP, Qiu R, Kitzman JO, Shendure J: **Chromosome-scale scaffolding of de novo genome assemblies based on chromatin interactions.** *Nature biotechnology* 2013, **31**:1119.

920 15. Kaplan N, Dekker J: **High-throughput genome scaffolding from in vivo DNA interaction frequency.** *Nature biotechnology* 2013, **31**:1143.

921 16. Lam ET, Hastie A, Lin C, Ehrlich D, Das SK, Austin MD, Deshpande P, Cao H, Nagarajan N, Xiao M: **Genome mapping on nanochannel arrays for structural variation analysis and sequence assembly.** *Nature biotechnology* 2012, **30**:771.

922 17. Avni R, Nave M, Barad O, Baruch K, Twardziok SO, Gundlach H, Hale I, Mascher M, Spannagl M, Wiebe K, et al: **Wild emmer genome architecture and diversity elucidate wheat evolution and domestication.** *Science* 2017, **357**:93-97.

923 18. Zhu T, Wang L, Rodriguez JC, Deal KR, Avni R, Distelfeld A, McGuire PE, Dvorak J, Luo MC: **Improved Genome Sequence of Wild Emmer Wheat Zavitan with the Aid of Optical Maps.** *G3 (Bethesda)* 2019, **9**:619-624.

924 19. Callaway E: **Small group scoops international effort to sequence huge wheat genome.** *Nature News* 2017.

925 20. Clavijo BJ, Venturini L, Schudoma C, Accinelli GG, Kaithakottil G, Wright J, Borrill P, Kettleborough G, Heavens D, Chapman H: **An improved assembly and annotation of the allohexaploid wheat genome identifies complete families of agronomic genes and provides genomic evidence for chromosomal translocations.** *Genome research* 2017, **27**:885-896.

926 21. Zimin AV, Puiu D, Luo MC, Zhu T, Koren S, Marcais G, Yorke JA, Dvorak J, Salzberg SL: **Hybrid assembly of the large and highly repetitive genome of Aegilops tauschii, a progenitor of bread wheat, with the MaSuRCA mega-reads algorithm.** *Genome Res* 2017, **27**:787-792.

927 22. Zimin AV, Puiu D, Hall R, Kingan S, Clavijo BJ, Salzberg SL: **The first near-complete assembly of the hexaploid bread wheat genome, *Triticum aestivum*.** *Gigascience* 2017.

928 23. Monat C, Schreiber M, Stein N, Mascher M: **Prospects of pan-genomics in barley.** *Theoretical and Applied Genetics* 2018:1-12.

929 24. International Wheat Genome Sequencing Consortium: **Shifting the limits in wheat research and breeding using a fully annotated reference genome.** *Science* 2018, **361**:eaar7191.

930 25. Zhang J, Koberst K, Flouri T, Stamatakis A: **PEAR: a fast and accurate Illumina Paired-End reAd mergeR.** *Bioinformatics* 2014, **30**:614-620.

931 26. Bushnell B, Rood J, Singer E: **BBMerge - Accurate paired shotgun read merging via overlap.** *PLoS One* 2017, **12**:e0185056.

932 27. Li H: **BFC: correcting Illumina sequencing errors.** *Bioinformatics* 2015, **31**:2885-2887.

933 28. Melsted P, Halldorsson BV: **KmerStream: streaming algorithms for k-mer abundance estimation.** *Bioinformatics* 2014, **30**:3541-3547.

934 29. Chikhi R, Limasset A, Medvedev P: **Compacting de Bruijn graphs from sequencing data quickly and in low memory.** *Bioinformatics* 2016, **32**:i201-i208.

935 30. Chikhi R, Rizk G: **Space-efficient and exact de Bruijn graph representation based on a Bloom filter.** *Algorithms Mol Biol* 2013, **8**:22.

936 31. Team RC: **R: A language and environment for statistical computing.** R Foundation for Statistical Computing, Vienna, Austria. 2016. 2017.

937 32. Sahlin K, Chikhi R, Arvestad L: **Assembly scaffolding with PE-contaminated mate-pair libraries.** *Bioinformatics* 2016, **32**:1925-1932.

967 33. Ghurye J, Pop M, Koren S, Bickhart D, Chin CS: **Scaffolding of long read assemblies**
968 **using long range contact information.** *BMC Genomics* 2017, **18**:527.

969 34. Beier S, Himmelbach A, Colmsee C, Zhang X-Q, Barrero RA, Zhang Q, Li L, Bayer M,
970 Bolser D, Taudien S, et al: **Construction of a map-based reference genome sequence**
971 **for barley, *Hordeum vulgare* L.** *Scientific Data* 2017, **4**:170044.

972 35. Lu F-H, McKenzie N, Kettleborough G, Heavens D, Clark MD, Bevan MW:
973 **Independent assessment and improvement of wheat genome sequence assemblies**
974 **using Fosill jumping libraries.** *GigaScience* 2018, **7**:giy053.

975 36. Li H: **Minimap2: pairwise alignment for nucleotide sequences.** *Bioinformatics* 2018,
976 **1**:7.

977 37. Mochida K, Yoshida T, Sakurai T, Ogihara Y, Shinozaki K: **TriFLDB: a database of**
978 **clustered full-length coding sequences from Triticeae with applications to**
979 **comparative grass genomics.** *Plant Physiol* 2009, **150**:1135-1146.

980 38. Wicker T, Sabot F, Hua-Van A, Bennetzen JL, Capy P, Chalhoub B, Flavell A, Leroy P,
981 Morgante M, Panaud O, et al: **A unified classification system for eukaryotic**
982 **transposable elements.** *Nature Reviews Genetics* 2007, **8**:973.

983 39. International Barley Genome Sequencing Consortium: **A physical, genetic and**
984 **functional sequence assembly of the barley genome.** *Nature* 2012, **491**:711.

985 40. Schnable PS, Ware D, Fulton RS, Stein JC, Wei F, Pasternak S, Liang C, Zhang J, Fulton
986 L, Graves TA: **The B73 maize genome: complexity, diversity, and dynamics.** *science*
987 2009, **326**:1112-1115.

988 41. Putnam NH, O'Connell BL, Stites JC, Rice BJ, Blanchette M, Calef R, Troll CJ, Fields A,
989 Hartley PD, Sugnet CW: **Chromosome-scale shotgun assembly using an in vitro**
990 **method for long-range linkage.** *Genome research* 2016.

991 42. Simao FA, Waterhouse RM, Ioannidis P, Kriventseva EV, Zdobnov EM: **BUSCO:**
992 **assessing genome assembly and annotation completeness with single-copy**
993 **orthologs.** *Bioinformatics* 2015, **31**:3210-3212.

994 43. Joyce BL, Haug-Batzell AK, Hulvey JP, McCarthy F, Devisetty UK, Lyons E: **Leveraging**
995 **CyVerse Resources for De Novo Comparative Transcriptomics of Underserved (Non-**
996 **model) Organisms.** *J Vis Exp* 2017.

997 44. Schmutz T, Bolger ME, Rudd S, Chen J, Gundlach H, Arend D, Oppermann M, Weise
998 S, Lange M, Spannagl M, et al: **Bioinformatics in the plant genomic and phenomic**
999 **domain: The German contribution to resources, services and perspectives.** *J*
1000 *Biotechnol* 2017, **261**:37-45.

1001 45. Toor S, Lindberg M, Falman I, Vallin A, Mohill O, Freyhult P, Nilsson L, Agback M,
1002 Viklund L, Zazzik H, et al: **SNIC Science Cloud (SSC): A National-Scale Cloud**
1003 **Infrastructure for Swedish Academia.** In *2017 IEEE 13th International Conference on*
1004 *e-Science (e-Science); 24-27 Oct. 2017.* 2017: 219-227.

1005 46. Yu G, Champouret N, Steuernagel B, Olivera PD, Simmons J, Williams C, Johnson R,
1006 Moscou MJ, Hernandez-Pinzon I, Green P, et al: **Discovery and characterization of**
1007 **two new stem rust resistance genes in *Aegilops sharonensis*.** *Theor Appl Genet*
1008 2017, **130**:1207-1222.

1009 47. Huang S, Steffenson BJ, Sela H, Stinebaugh K: **Resistance of *Aegilops longissima* to**
1010 **the Rusts of Wheat.** *Plant Dis* 2018, **102**:1124-1135.

1011 48. Geiger H, Miedaner T: **Rye breeding.** *Cereals* 2009, **3**:157-181.

1012 49. Bauer E, Schmutz T, Barilar I, Mascher M, Gundlach H, Martis MM, Twardziok SO,
1013 Hackauf B, Gordillo A, Wilde P: **Towards a whole-genome sequence for rye (*Secale***

1014 *cereale* L.). *The Plant Journal* 2017, **89**:853-869.

1015 50. Hirsch C, Hirsch CD, Brohammer AB, Bowman MJ, Soifer I, Barad O, Shem-Tov D,
1016 Baruch K, Lu F, Hernandez AG: **Draft assembly of elite inbred line PH207 provides**
1017 **insights into genomic and transcriptome diversity in maize.** *The Plant Cell* 2016:tpc.
1018 00353.02016.

1019 51. Springer NM, Anderson SN, Andorf CM, Ahern KR, Bai F, Barad O, Barbazuk WB, Bass
1020 HW, Baruch K, Ben-Zvi G, et al: **The maize W22 genome provides a foundation for**
1021 **functional genomics and transposon biology.** *Nat Genet* 2018, **50**:1282-1288.

1022 52. Unterseer S, Seidel MA, Bauer E, Haberer G, Hochholdinger F, Opitz N, Marcon C,
1023 Baruch K, Spannagl M, Mayer KFX, Schön C-C: **European Flint reference sequences**
1024 **complement the maize pan-genome.** *bioRxiv* 2017:103747.

1025 53. Thind AK, Wicker T, Simkova H, Fossati D, Moullet O, Brabant C, Vrana J, Dolezel J,
1026 Krattinger SG: **Rapid cloning of genes in hexaploid wheat using cultivar-specific**
1027 **long-range chromosome assembly.** *Nat Biotechnol* 2017, **35**:793-796.

1028 54. Wendler N, Mascher M, Himmelbach A, Johnston P, Pickering R, Stein N: **Bulbosum**
1029 **to go: a toolbox to utilize *Hordeum vulgare*/bulbosum introgressions for breeding**
1030 **and beyond.** *Molecular plant* 2015, **8**:1507-1519.

1031 55. Xue S, Kolmer JA, Wang S, Yan L: **Mapping of Leaf Rust Resistance Genes and**
1032 **Molecular Characterization of the 2NS/2AS Translocation in the Wheat Cultivar**
1033 **Jagger.** *G3 (Bethesda)* 2018, **8**:2059-2065.

1034 56. Jiao Y, Peluso P, Shi J, Liang T, Stitzer MC, Wang B, Campbell MS, Stein JC, Wei X, Chin
1035 CS, et al: **Improved maize reference genome with single-molecule technologies.**
1036 *Nature* 2017, **546**:524-527.

1037 57. Schmidt MH, Vogel A, Denton AK, Istance B, Wormit A, van de Geest H, Bolger ME,
1038 Alseekh S, Mass J, Pfaff C, et al: **De Novo Assembly of a New *Solanum pennellii***
1039 **Accession Using Nanopore Sequencing.** *Plant Cell* 2017, **29**:2336-2348.

1040 58. Wang M, Tu L, Yuan D, Zhu, Shen C, Li J, Liu F, Pei L, Wang P, Zhao G, et al: **Reference**
1041 **genome sequences of two cultivated allotetraploid cottons, *Gossypium hirsutum***
1042 **and *Gossypium barbadense*.** *Nat Genet* 2019, **51**:224-229.

1043 59. Wenger AM, Peluso P, Rowell WJ, Chang P-C, Hall RJ, Concepcion GT, Ebler J,
1044 Fungtammasan A, Kolesnikov A, Olson ND, et al: **Highly-accurate long-read**
1045 **sequencing improves variant detection and assembly of a human genome.** *bioRxiv*
1046 2019:519025.

1047 60. Martin M: **Cutadapt removes adapter sequences from high-throughput sequencing**
1048 **reads.** *EMBnet Journal* 2011, **17**:pp. 10-12.

1049 61. O'Connell J, Schulz-Trieglaff O, Carlson E, Hims MM, Gormley NA, Cox AJ: **NxTrim:**
1050 **optimized trimming of Illumina mate pair reads.** *Bioinformatics* 2015, **31**:2035-2037.

1051 62. Luo R, Liu B, Xie Y, Li Z, Huang W, Yuan J, He G, Chen Y, Pan Q, Liu Y: **SOAPdenovo2:**
1052 **an empirically improved memory-efficient short-read de novo assembler.**
1053 *Gigascience* 2012, **1**:18.

1054 63. Li H, Handsaker B, Wysoker A, Fennell T, Ruan J, Homer N, Marth G, Abecasis G,
1055 Durbin R: **The sequence alignment/map format and SAMtools.** *Bioinformatics* 2009,
1056 **25**:2078-2079.

1057 64. Quinlan AR, Hall IM: **BEDTools: a flexible suite of utilities for comparing genomic**
1058 **features.** *Bioinformatics* 2010, **26**:841-842.

1059 65. Csardi G, Nepusz T: **The igraph software package for complex network research.**
1060 *InterJournal, Complex Systems* 2006, **1695**:1-9.

1061 66. Rice P, Longden I, Bleasby A: **EMBOSS: the European molecular biology open**
1062 **software suite.** *Trends in genetics* 2000, **16**:276-277.

1063 67. Li H: **Aligning sequence reads, clone sequences and assembly contigs with BWA-MEM.** *arXiv preprint arXiv:13033997* 2013.

1064 68. Hu M, Deng K, Selvaraj S, Qin Z, Ren B, Liu JS: **HiCNorm: removing biases in Hi-C data via Poisson regression.** *Bioinformatics* 2012, **28**:3131-3133.

1065 69. Putnam NH, O'Connell BL, Stites JC, Rice BJ, Blanchette M, Calef R, Troll CJ, Fields A, Hartley PD, Sugnet CW, et al: **Chromosome-scale shotgun assembly using an in vitro method for long-range linkage.** *Genome Res* 2016, **26**:342-350.

1066 70. Wu TD, Watanabe CK: **GMAP: a genomic mapping and alignment program for mRNA and EST sequences.** *Bioinformatics* 2005, **21**:1859-1875.

1067 71. Gremme G, Brendel V, Sparks ME, Kurtz S: **Engineering a software tool for gene structure prediction in higher organisms.** *Information and Software Technology* 2005, **47**:965-978.

1068 72. Matsumoto T, Tanaka T, Sakai H, Amano N, Kanamori H, Kurita K, Kikuta A, Kamiya K, Yamamoto M, Ikawa H, et al: **Comprehensive sequence analysis of 24,783 barley full-length cDNAs derived from 12 clone libraries.** *Plant Physiol* 2011, **156**:20-28.

1069 73. Kim D, Langmead B, Salzberg SL: **HISAT: a fast spliced aligner with low memory requirements.** *Nat Methods* 2015, **12**:357-360.

1070 74. Pertea M, Pertea GM, Antonescu CM, Chang TC, Mendell JT, Salzberg SL: **StringTie enables improved reconstruction of a transcriptome from RNA-seq reads.** *Nat Biotechnol* 2015, **33**:290-295.

1071 75. Ghosh S, Chan CK: **Analysis of RNA-Seq Data Using TopHat and Cufflinks.** *Methods Mol Biol* 2016, **1374**:339-361.

1072 76. Altschul SF, Gish W, Miller W, Myers EW, Lipman DJ: **Basic local alignment search tool.** *J Mol Biol* 1990, **215**:403-410.

1073 77. Eddy SR: **Accelerated Profile HMM Searches.** *PLoS Comput Biol* 2011, **7**:e1002195.

1074 78. Stanke M, Schoffmann O, Morgenstern B, Waack S: **Gene prediction in eukaryotes with a generalized hidden Markov model that uses hints from external sources.** *BMC Bioinformatics* 2006, **7**:62.

1075 79. Haas BJ, Salzberg SL, Zhu W, Pertea M, Allen JE, Orvis J, White O, Buell CR, Wortman JR: **Automated eukaryotic gene structure annotation using EVidenceModeler and the Program to Assemble Spliced Alignments.** *Genome Biol* 2008, **9**:R7.

1076 80. Spannagl M, Nussbaumer T, Bader KC, Martis MM, Seidel M, Kugler KG, Gundlach H, Mayer KF: **PGSB PlantsDB: updates to the database framework for comparative plant genome research.** *Nucleic Acids Res* 2016, **44**:D1141-1147.

1077 81. Ellinghaus D, Kurtz S, Willhöft U: **LTRharvest, an efficient and flexible software for de novo detection of LTR retrotransposons.** *BMC Bioinformatics* 2008, **9**:18.

1078 82. Mistry J, Finn RD, Eddy SR, Bateman A, Punta M: **Challenges in homology search: HMMER3 and convergent evolution of coiled-coil regions.** *Nucleic Acids Res* 2013, **41**:e121.

1079 83. SanMiguel P, Gaut BS, Tikhonov A, Nakajima Y, Bennetzen JL: **The paleontology of intergene retrotransposons of maize.** *Nat Genet* 1998, **20**:43-45.

1080 84. Benson G: **Tandem repeats finder: a program to analyze DNA sequences.** *Nucleic Acids Res* 1999, **27**:573-580.

1081 85. Kurtz S, Narechania A, Stein JC, Ware D: **A new method to compute K-mer frequencies and its application to annotate large repetitive plant genomes.** *BMC Genomics* 2008, **9**:517.

1109 86. Wicker T, Yu Y, Haberer G, Mayer KF, Marri PR, Rounsley S, Chen M, Zuccolo A,
1110 Panaud O, Wing RA, Roffler S: **DNA transposon activity is associated with increased**
1111 **mutation rates in genes of rice and other grasses.** *Nat Commun* 2016, **7**:12790.

1112 87. Arend D, Junker A, Scholz U, Schüler D, Wylie J, Lange M: **PGP repository: a plant**
1113 **phenomics and genomics data publication infrastructure.** *Database* 2016, **2016**.

1114 88. Arend D, Lange M, Chen J, Colmsee C, Flemming S, Hecht D, Scholz U: **e! DAL-a**
1115 **framework to store, share and publish research data.** *BMC bioinformatics* 2014,
1116 **15**:214.

1117 89. Tange O: **Gnu parallel-the command-line power tool.** *The USENIX Magazine* 2011,
1118 **36**:42-47.

1119 90. Himmelbach A, Walde I, Mascher M, Stein N: **Tethered Chromosome Conformation**
1120 **Capture Sequencing in Triticeae: A Valuable Tool for Genome Assembly.** *Bio-*
1121 *protocol* 2018, **8**:e2955.

1122 91. S P, A H, M M, N S: **In situ Hi-C for plants: an improved method to detect long-range**
1123 **chromatin interactions.** In *Plant long non-coding RNAs: methods and protocols*.
1124 Edited by J C, H-L W. New York, NY; 2019: *Methods in molecular biology*].

1125 92. Mohamadi H, Khan H, Birol I: **ntCard: a streaming algorithm for cardinality**
1126 **estimation in genomics data.** *Bioinformatics* 2017, **33**:1324-1330.

1127 93. Himmelbach A, Ruban A, Walde I, Šimková H, Doležel J, Hastie A, Stein N, Mascher M:
1128 **Discovery of multi-megabase polymorphic inversions by chromosome**
1129 **conformation capture sequencing in large-genome plant species.** *The Plant Journal*
1130 2018.

1131